ACUT$_2$E TSE-SSFP: A Hybrid Method for T2-Weighted Imaging of Edema in the Heart

Anthony H. Aletras,* Peter Kellman, J. Andrew Derbyshire, and Andrew E. Arai

ACUT$_2$E TSE-SSFP is a hybrid between steady state free precession (SSFP) and turbo spin echo (TSE) for bright-blood T2-weighted imaging with signal-to-noise ratio (SNR) and contrast-to-noise ratio (CNR) similar to dark-blood TSE. TSE-SSFP uses a segmented SSFP readout during diastole with 180° pulses following a 90° preparation. The 180° refocusing pulses make TSE-SSFP similar to TSE but TSE-SSFP uses gradient moment nulling, whereas TSE uses gradient crushing. TSE-SSFP produced T2-weighted images with minimal T1 weighting. TSE-SSFP and TSE had similar SNR (155.9 ± 6.0 vs 160.9 ± 7.0; *P* = NS) for acute myocardial infarction (MI) and twice the SNR of T2-prepared SSFP (73.1 ± 3.4, *P* < 0.001). TSE-SSFP and TSE had approximately double the CNR of T2-prepared SSFP for differentiating acute MI from normal myocardium. Imperfect blood suppression, present in all animals on some TSE images, was a problem eliminated by TSE-SSFP and T2-prepared SSFP. **Magn Reson Med 59:229–235, 2008.** © 2008 Wiley-Liss, Inc.

Key words: Edema; infarction; T2; ACUT$_2$E; ACUTE; C-TIDE; myocardium; heart

T2-weighted turbo spin echo (TSE) (1) cardiac MRI of edema has recently received attention for transplant rejection (2), for differentiating acute versus chronic myocardial infarction (3), for identifying patients with acute myocarditis (4) and for in vivo delineation of the ischemic area at risk in acute myocardial infarction (5). T2-weighted imaging of edema provides complementary information to that obtained by delayed contrast enhanced MRI (6) of infarction and fibrosis. While the current clinical standard T2-weighted dark-blood TSE (7) has been instrumental in imaging edema associated with such pathology, the dark-blood preparation leaves residual bright rim blood artifacts next to the endocardium due to inadequate suppression of the signal from the blood pool and is limited by posterior wall signal losses associated with improper timing. Such timing imperfections between the dark-blood preparation and the TSE acquisition result in through-plane motion of the dark-blood prepared slice out of the TSE imaging slice (8). The latter has been recently addressed by specialized techniques aiming to improve acquisition timing (9). With commonly available dark-blood TSE methods decreasing

the double inversion slab thickness accentuates the posterior wall signal losses whereas increasing the slab thickness results in more pronounced bright rim artifacts. Steady state free precession (SSFP, a.k.a. true FISP, FIESTA, balanced-FFE) (10) with a T2 preparation (T2P-SSFP) was recently introduced to successfully address these issues and improve diagnostic accuracy (11) albeit at reduced signal-to-noise ratio (SNR).

Our aim was to develop ACUT$_2$E imaging (Acquisition for Cardiac Unified T2 Edema), a TSE-SSFP hybrid method for T2-weighted cardiac imaging of edema associated with acute myocardial infarction. Such a hybrid method could combine the inherent bright-blood contrast of an SSFP acquisition with the T2-weighting and the higher contrast-to-noise ratio (CNR) inherent to TSE. We hypothesized that single cardiac phase TSE-SSFP images would possess T2-weighting and bright-blood contrast. We also hypothesized that TSE-SSFP would possess in vivo SNR and CNR similar to that of dark-blood TSE and higher than what can be obtained with T2P-SSFP. We specifically developed this methodology to improve imaging of T2-weighted abnormalities associated with acute myocardial infarction, myocarditis, and possibly transplant rejection.

MATERIALS AND METHODS

MRI

The pulse sequence diagram of conventional TSE is shown in Figure 1A preceded by a double inversion recovery preparation to improve black blood contrast (7). The TSE readout uses 180° refocusing pulses to form a train of spin echoes and is usually gated during diastole to minimize cardiac motion artifacts. Gradient crushers bracketing the 180° pulses ensure that magnetization experiencing less than a perfect 180° nutation is crushed. T2 contrast is obtained by a proper phase encode ordering scheme (7), which fills the center of *k*-space with echoes from the desired effective echo time (TE).

Recently (11), T2-prepared SSFP (T2P-SSFP) was proposed for imaging edema with bright-blood contrast (Fig. 1B). A T2 preparation, consisting of nonselective 180° refocusing pulses, establishes T2 contrast (12). The T2 prepared magnetization is then stored along the longitudinal axis. SSFP imaging with flip angles up to 90° is used to read out the prepared magnetization. The SSFP is by nature fully gradient moment balanced and as such phase coherence is preserved among successive repetitions (TRs). To accelerate the transition into steady state, either an α/2-TR/2 introduction (13) or a linear ramp flip (14) can
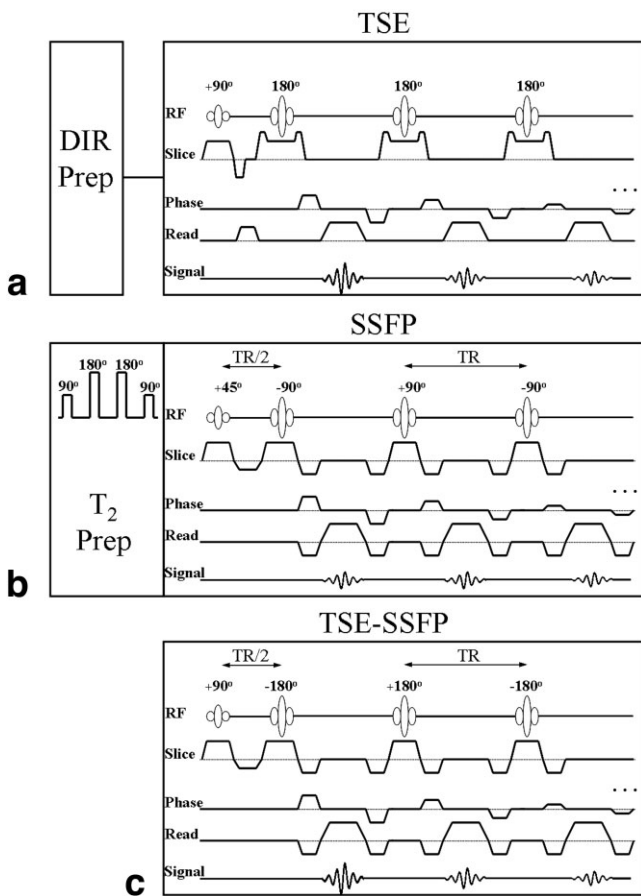
FIG. 1. **A:** Dark-blood TSE pulse sequence diagram. A double inversion recovery (DIR) preparation is applied upon detecting the R-wave of the electrocardiogram to suppress moving blood. The readout consists of consecutive 180° refocusing pulses which create spins echoes during diastole. Gradient crushers are used as part of the refocusing process to eliminate signal not originating from the initial excitation (90°). **B:** T2P-SSFP pulse sequence diagram. The T2-preparation is responsible for the majority of the T2 contrast. The SSFP readout has some additional T2 and T1 contrast (28). **C:** ACUT$_2$E imaging TSE-SSFP pulse sequence diagram. T2-contrast is created by the SSFP readout itself through the use of 180° refocusing pulses and a linear phase ordering scheme. The use of 180° refocusing pulses reduces the SSFP T1 contrast mechanism and results in a primarily T2-weighted image. ACUT$_2$E TSE-SSFP is a hybrid between TSE and SSFP.

be used. A linear ramp flip with 10 radio frequency (RF) pulses was used in this study for its better off-resonance performance (14).

The ACUT$_2$E imaging TSE-SSFP pulse sequence diagram is shown in Figure 1C. This is an SSFP readout with flip angles α of 180° with the readout gated during diastole. Note the similarities of this readout with the readout part of the T2P-SSFP method (Fig. 1B). However, TSE-SSFP does not require a black-blood preparation or a T2-preparation. An α/2-TR/2 introduction ensures immediate transition into driven equilibrium (13,15). The gradient moment nulling, inherent to SSFP, results in preserved phase coherence between successive repetitions. The use of refocusing 180° pulses makes this pulse sequence also similar to the TSE readout (Fig. 1A), because spin echoes are generated (16). An important difference between the two methods is that TSE-SSFP uses gradient moment nulling similar to that described for TSE by Hinks and Constable (17) whereas the conventional TSE implementation uses gradient crushing. TSE-SSFP thus creates a coherent train of spin echoes that are inherently T2-weighted (17,18). This is unlike low flip angle SSFP readout schemes that possess both T2 and T1 contrast (19). TSE-SSFP with proper phase encode ordering (see below) will yield images with T2 contrast.

Imaging was performed at 1.5 Tesla (T) with an Avanto MRI scanner (Siemens Medical Solutions, Erlangen, Germany) with a Nova Medical Systems (Wilmington, MA) eight-channel phased-array coil. Each of the three imaging methods was gated to the electrocardiogram to obtain a single diastolic image per breathhold. MRI parameters are depicted in Table 1. To make the comparison relevant in terms of SNR per unit time, the receiver bandwidths were adjusted so as to maintain the same echo train duration for all three methods. As a result, the receiver bandwidths of TSE-SSFP and T2P-SSFP were higher than that of TSE. This finding is because the SSFP moment-nulling rephasing gradient pulses take more time to play out than the TSE crusher gradient pulses due to the additional ramps involved. Therefore, data points had to be acquired faster with SSFP to compensate for this slower application of gradient pulses. Comparisons of SNR and CNR used an effective TE of 60 ms for all methods.

For T2P-SSFP images an MLEV-4 (20) (decoupling four-step phase cycling) scheme was used to improve the performance of the T2 preparation as previously described (11,12). A proton density-weighted gradient echo image was acquired interleaved with the T2-weighted acquisition every other heartbeat. This image was used for surface coil intensity correction.

Table 1
MRI Parameters

	Matrix	Voxel (mm^3)	Repetition (heartbeats)	Flip angle (degrees)	ESP or TR (ms)	ETL or VPS	Readout (ms)	Bandwidth (Hz/pixel)	Averages	Acquisition time (s)
TSE	192x125	1.5x1.5x6	3–6	180	3.6	25	90ms	798	1	16–18
T2P-SSFP	192x125	1.5x1.5x6	3–6	90	3.6	25	90ms	960	1	13–15
TSE-SSFP	192x125	1.5x1.5x6	3–6	180	3.6	25	90ms	960	1	13–15

ETL = echotrain length; VPS = views per segment; Bandwidth = receiver bandwidth (adjusted to obtain identical echotrain durations for all three methods); ESP = echo spacing; TR = repetition time.

For TSE-SSFP, twenty-five 180° pulses were used during the readout. The number of dummy 180° pulses (N) followed the 90° RF pulse, that is, $90°\text{-}(180°)_{\times N}\text{-}(180°)_{\times 25}$. Along with linear *k*-space ordering, this strategy allowed for adjusting the effective echo time to the desired value (N = 0−66 yielding echo times of 47−286 ms). A proton density-weighted gradient echo image was also acquired as with T2P-SSFP.

Because signal from adipose tissue is usually higher than that of edematous myocardium and can be easily differentiated from edema, fat STIR suppression (7) was not used so as to avoid the additional signal losses associated with a third inversion pulse and also to avoid the undesirable T1-weighting. Last, chemical shift-based fat suppression is not commonly applied for T2-weighted cardiac MRI with modern short bore magnets where static field inhomogeneity can vary significantly, and insufficient shimming (e.g., due to sternal wires) can result in unpredictable direct saturation of the myocardial signal across space. To localize the infarcted zone independently of the T2-weighted imaging, standard delayed contrast enhancement was performed with Gd-DTPA approximately 10−15 min after intravenous contrast medium infusion as described previously (5).

Simulations

Simulations were used to obtain a step-wise integration of the Bloch equations. The simulations used a four-vector formalism (21), thus allowing for T1 and T2 relaxations B1, B0 and the selection of transmitter or receiver phases, to be expressed as a 4 × 4 matrix operator. These were combined to provide a transition matrix from one echo to the next.

For each pulse sequence, the magnetization was tracked at multiple points across the slice profile. RF pulses were emulated using the actual pulse B1 profiles obtained from the scanner. The simulated signal at each echo was obtained by identifying the transverse magnetization as a complex value and integrating over the slice profile.

Phantoms

Agar phantoms with $CuSO_4$ were used to approximate characteristics of normal myocardium (T1 = 813 ms, T2 = 49 ms, referred to as "Normal") and edematous myocardium (T1 = 882 ms, T2 = 65 ms, referred to as "Edema"; 11,22). A third phantom (T1 = 158 ms, T2 = 48 ms) was selected to demonstrate the T1 independence of TSE-SSFP. Phantom T2s were measured with spin-echo imaging (TR 6 s, TE 5.5−600 ms, one echo per TR) whereas T1s were measured with inversion recovery imaging (TR 6 s, TI 76−2800 ms).

Animal Preparation

All animal experiments were approved by the Animal Care and Use Committee of the National Heart, Lung and Blood Institute of the National Institutes of Health. Eight dogs were anesthetized with subcutaneous administration of acepromazine (0.2 mg/kg), intravenous administration of thiopental sodium (15 mg/kg), and inhaled isoflurane (0.5−2.0%). Surgical preparation included a left jugular 8-F Hickman catheter, a left atrial appendage infusion catheter (Broviac 6.6F), a femoral arterial line, and an occluder around the left anterior descending (LAD) coronary artery usually distal to the first diagonal branch. A 90-min total LAD occlusion was performed, to induce myocardial infarction, followed by reperfusion as previously described (5). Imaging was performed 3 days after infarction.

Statistics and Measurement of SNR and CNR

Noise was estimated from the T2-weighted images using the standard deviation and the mean of a large region of interest in an area outside the phantoms or the animal as previously described (23). This approach was possible because parallel imaging was not applied (however, all three methods are compatible with parallel acceleration). SNR (23) and CNR (difference between two SNR values) were measured based on regions of interest placed in the anterior wall within the LAD coronary distribution (defined as "Edema") and in the inferior wall (defined as "Normal"). Surface coil intensity correction was performed by computing the ratio of the mean signal intensities of "Edema" divided by "Normal" from a proton density weighted image. The mean signal intensity of "Normal" of the T2-weighted image was then multiplied by this sensitivity ratio to correct for the surface coil drop off. Region of interest (ROI) placement in the LAD territory was based on the delayed enhanced images for identifying the infarcted zone. The ROI within the LV blood pool was placed adjacent to the LAD ROI. SNR and CNR statistical comparisons between the three imaging methods were performed with paired *t*-tests with Bonferroni correction for multiple comparisons.

RESULTS

Simulation Data

The simulated signal versus TE is shown in Figure 2. For TSE (Fig. 2A), the true T2 values ($T2_{normal}$ = 49 ms and $T2_{edema}$ = 65 ms) were overestimated ($T2_{normal}$ = 57 and $T2_{edema}$ = 75 ms). Overestimation was also present with TSE-SSFP (Fig. 2B; $T2_{normal}$ = 68 and $T2_{edema}$ = 87 ms) whereas T2-prepared SSFP (Fig. 2C) yielded the true T2 values within a fraction of a millisecond. Note that, with TSE-SSFP (Fig. 2B), the signal decay does not asymptotically reach zero due to imperfections in the slice profile, which force spins that experience the lower flip angle to a steady state condition. Also, due to the lower flip angle used with T2-prepared SSFP the decay curve intersects with the *y*-axis at lower signal values (Fig. 2C) compared with TSE-SSFP (Fig. 2B).

Phantom Data

T2 contrast was observed between the "normal" and "edema" phantoms with spin echo, TSE, TSE-SSFP, and T2P-SSFP as qualitatively obvious differences in signal intensity. Measurement of T2 in the phantoms reveals subtler differences between the techniques. T2 in the agar phantoms, as measured with a fully T1 relaxed spin echo, was $T2_{normal}$ = 49 ms and $T2_{edema}$ = 65 ms. The spin-echo acquisition with long TRs (6 s) for full T1 relaxation al-
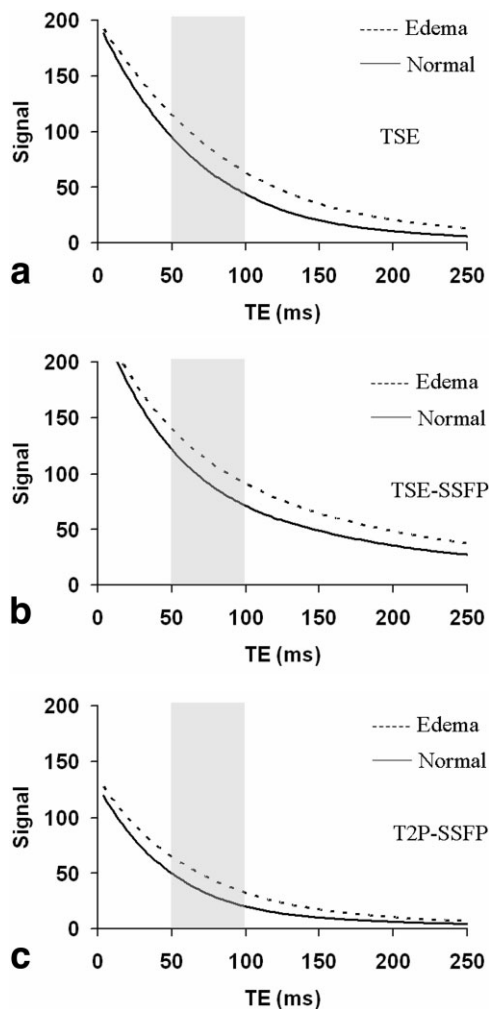
FIG. 2. **A:** TSE overestimated the T2 values of "normal" and "edema" tissues in this simulation. The signal for both tissues drops asymptotically to zero as expected. The gray area marks the range of physiologically relevant echo times for edema imaging in the heart. Note that the axes have been scaled similarly for A, B, and C. **B:** For ACUT$_2$E TSE-SSFP, the simulations predicted that the signal from the two tissues would be different within the range of physiologically relevant echo times for edema imaging (gray zone). Note that asymptotically the signal for both tissues does not reach zero due to the imperfect slice profile. Note that the axes have been scaled similarly for A, B, and C. **C:** For both tissues, the T2-prepared SSFP simulations showed reduced signal as a result of the lower readout flip angles. Physiologically relevant echo times for edema imaging are within the gray zone. The decay curve intersects with the y-axis at lower signal values compared with the TSE due to the lower readout flip angles of T2-prepared SSFP. Note that the axes have been scaled similarly for A, B, and C.

lowed for unequivocal determination of the T2 values for these two phantoms.

The T2 of the agar phantoms was also measured with TSE, T2P-SSFP, and TSE-SSFP. As with simulation data, TSE overestimated the T2 of the phantoms (T2$_{normal}$ = 57 ms and T2$_{edema}$ = 71 ms) perhaps as a result of the range of TEs examined (limited by the echotrain length) or specific details related to this product pulse sequence or due to the creation of stimulated echoes. TSE-SSFP also over-
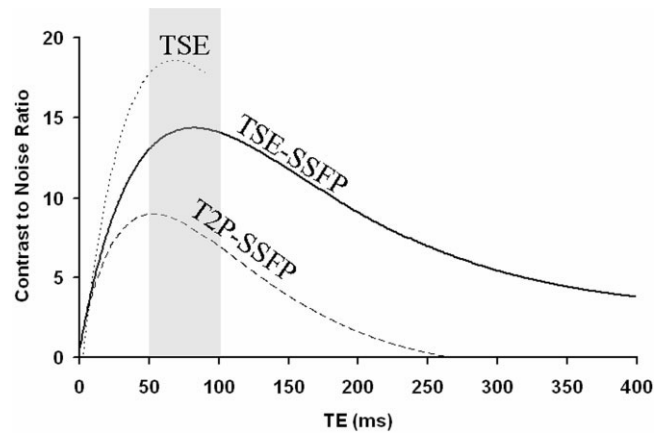

FIG. 3. ACUT$_2$E TSE-SSFP and TSE outperformed T2P-SSFP with respect to CNR in phantoms. CNRs were higher with dark-blood TSE than with TSE-SSFP as a result of the more efficient readout, which allowed for lower TSE receiver bandwidths.

estimated T2 values (T2$_{normal}$ = 65 ms and T2$_{edema}$ = 81 ms). T2 values measured with T2P-SSFP were T2$_{normal}$ = 49 ms and T2$_{edema}$ = 64 ms.

The CNR between "edema" and "normal" agar phantoms for all three methods is shown in Figure 3. All are plotted on the same y-scale for direct comparison. For echo
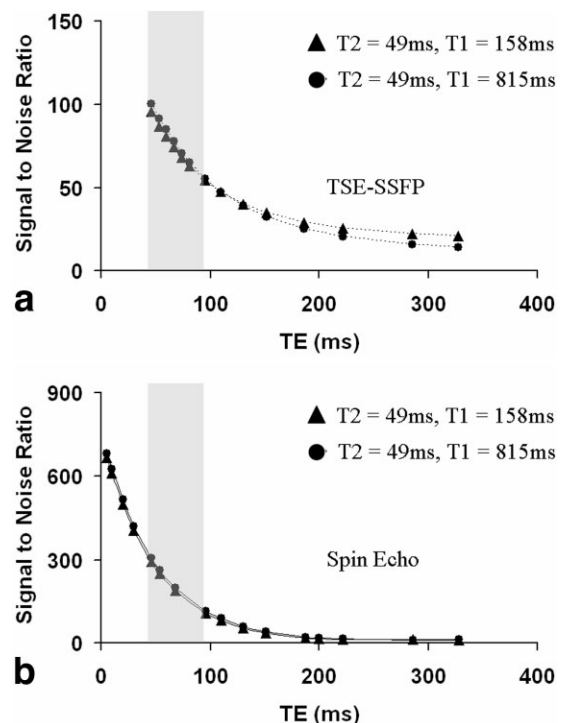

FIG. 4. **A:** Within the range of physiologically relevant echo times (gray areas), ACUT$_2$E TSE-SSFP is primarily T2-weighted with little T1 contrast. In phantoms with the same T2 constant, despite a fivefold change in T1s, the two T2 relaxation curves are almost superimposed within the gray area. **B:** As expected, the spin echo acquisition is primarily T2-weighted with little T1 contrast for every TE. In phantoms with the same T2 constant, despite a fivefold change in T1s, the two T2 relaxation curves are almost superimposed.
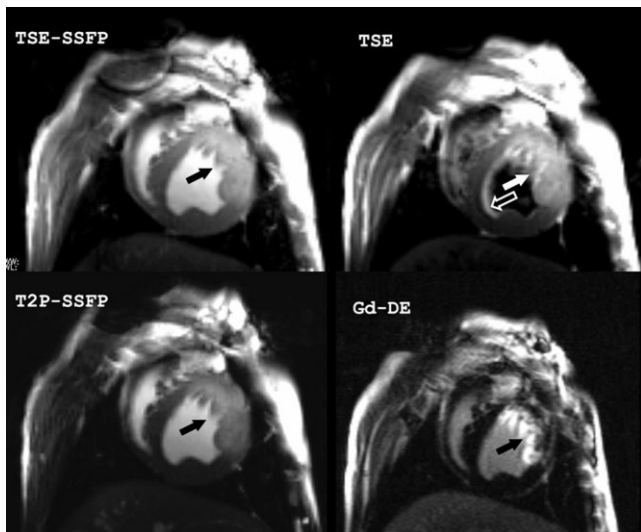
FIG. 5. With ACUT$_2$E TSE-SSFP, a transmural hyperintense zone (full arrow) is identified in the left anterior descending coronary artery territory where a subendocardial acute myocardial infarction is present (as seen in the Gd-DE viability image used for ROI selection, full arrow). The bright-blood contrast inherent to TSE-SSFP clearly depicts the endocardial border. With dark-blood TSE, the same area is identified (full arrow). However, due to incomplete blood suppression (open arrow), it is not easy to differentiate stagnant blood from edematous myocardium. T2P-SSFP has features similar to those of TSE-SSFP but with reduced SNR.

times relevant to edema imaging with cardiac MRI (gray area), TSE-SSFP yielded less CNR (by 25%) than that obtained with dark-blood TSE. However, TSE-SSFP outperformed T2P-SSFP by 55%. These values are within 15% to those predicted by first-order simulations.

TSE-SSFP is a T2-weighted imaging pulse sequence with little T1-weighting (Fig. 4A) where the SNR as a function of echo time between two phantoms of similar T2 (49 ms) and drastically different T1s (815 vs 158 ms) are depicted. Note that, for echo times relevant to imaging myocardial edema (gray area), the two curves almost overlap despite the more than fivefold change in T1. For comparison purposes, the spin echo data from the same phantoms are shown in Figure 4B. As expected, the spin echo data show little T1-weighting.

In Vivo Results for Acute Myocardial Infarction

Heart rate ranged from 85 to 140 beats per minute. Typical short axis views of the heart acquired from a dog 3 days after infarction with TSE-SSFP, dark-blood TSE, and T2P-SSFP are shown in Figure 5. As a reference, a viability image of the same slice with delayed gadolinium enhancement delineates the subendocardial infarct in the anterior region. TSE-SSFP, dark-blood TSE, and T2P-SSFP all identify a zone of hyperintensity associated with this infarct (full arrows). TSE-SSFP and T2P-SSFP possess bright-blood contrast, whereas dark-blood TSE suppresses most of the left ventricular blood signal. However, due to stagnant blood, incomplete blood suppression with TSE results in a bright subendocardial rim along the septum (open arrow), which compromises differentiation of blood

and edematous myocardium. In this study, such stagnant blood artifacts were seen in all eight animals with dark-blood TSE. For TSE-SSFP stagnant blood artifacts were not observed and the CNR between edematous myocardium and the immediately adjacent LV blood pool was 68.4 ± 10.4, suggesting that blood can be distinguished from edematous myocardium with high CNR.

In vivo, TSE and TSE-SSFP had similar SNR for edema associated with acute myocardial infarction (Fig. 6A; 155.9 ± 6.0 vs 160.9 ± 7.0; P = NS) and both had approximately twice the SNR of T2P-SSFP (73.1 ± 3.4, P < 0.001). The CNR between edematous and normal myocardium was not significantly different between TSE-SSFP and TSE, but both had twice the CNR of T2P-SSFP (Fig. 6B).

DISCUSSION

ACUT$_2$E TSE-SSFP is a new hybrid cardiac T2-weighted bright-blood imaging method with high SNR and CNR for imaging myocardial edema. Because TSE-SSFP is both a flow-compensated TSE (17) and an SSFP acquisition with 180° refocusing pulses (10), it bridges the gap between fully balanced SSFP pulse sequences and multi-echo spin echo techniques (24), thus unifying these two categories of pulse sequences into one. The spin physics of both gradient moment nulled TSE and T2-weighted transition into
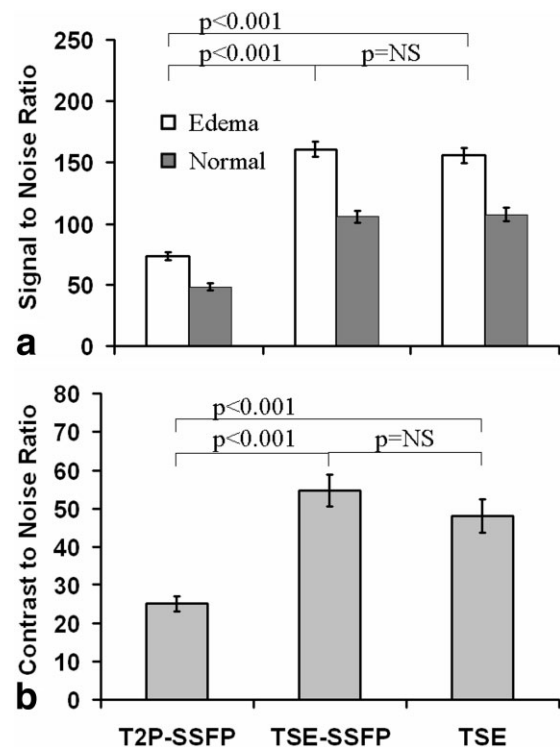

FIG. 6. **A:** Results from all animals imaged with TE = 60 ms, ACUT$_2$E TSE-SSFP and TSE yield roughly twice the SNR as T2P-SSFP. Error bars depict the standard error of the mean, which provides a measure of the accuracy of the estimates. **B:** In vivo, TSE-SSFP and TSE possessed significantly higher CNR compared to T2P-SSFP (P < 0.001). Error bars depict the standard error of the mean, which provides a measure of the accuracy of the estimates.

driven equilibrium (TIDE) have been described in detail in the past (17,18) and explain the T2 contrast mechanisms of TSE-SSFP. ACUT$_2$E TSE-SSFP uses the TIDE as previously described by Hennig et al. (15). The originally proposed T2-weighted TIDE (18) used variable flip angles, because it was geared toward applications with long acquisition windows; thus, RF specific absorption ratio limited the number of 180 degree readouts per unit time. In contrast, ACUT$_2$E TSE-SSFP is geared toward single cardiac phase imaging where rather short acquisition windows during diastole are used. Therefore, TSE-SSFP can use a complete train of 180 refocusing pulses throughout the data acquisition. This approach comes with certain benefits. While with TSE-SSFP the refocusing RF pulses are cycled in an SSFP-like manner between 0° and 180°, the exclusive use of refocusing pulses means that TSE-SSFP is otherwise similar to the gradient moment nulled TSE pulse sequence described by Hinks and Constable for imaging the spine (17). Therefore, for imaging edema associated with acute myocardial infarction, TSE-SSFP possesses desirable characteristics of TSE, such as T2-weighting with high CNR, in addition to the properties inherent to SSFP, such as bright-blood contrast. The current results also show that TSE-SSFP possesses high CNR between the edematous myocardium and the LV blood pool, so that the two can be distinguished without ambiguity.

Comparisons Between ACUT$_2$E TSE-SSFP and Dark-Blood TSE

Despite clinical usage based on feasibility within a breath-hold and adequate CNR, dark-blood TSE is limited by artifacts (8,11). Inadequate blood suppression occurred in all animals in this study with dark-blood TSE, a problem that worsens with increasing slice thickness. The gradient crushers bracketing the 180 refocusing pulses in TSE and the double inversion recovery preparation (7) suppress the signal from moving blood but neither works well for stagnant blood near wall motion abnormalities. The double inversion preparation introduces artifactual decreases in myocardial signal intensity when the TSE readout is not properly synchronized with the preparation. Methods to correct TSE for this problem have been proposed (9). Increasing the slab thickness of the dark-blood preparation to mitigate this problem usually results in more pronounced bright rim blood artifacts. TSE-SSFP fixes this problem. TSE does not accurately measure T2 as a result of diffusion, slice profile, k-space phase ordering, and possibly other mechanisms (25,26). T2 measurements are also distorted in TSE-SSFP as a result of similar mechanisms and potentially due to the asymptotic signal decay to non-zero values at long echo times. Nonetheless, TSE-SSFP provides diagnostic quality T2-weighted images. Last, the dark-blood preparation may introduce additional signal losses in vivo as a result motion or poor in vivo flip angle calibration for the double inversion RF pulses. This may explain why the theoretical bandwidth-related SNR advantage of TSE over TSE-SSFP was not observed in vivo.

Comparisons Between ACUT$_2$E TSE-SSFP and T2P-SSFP

While both TSE-SSFP and T2P-SSFP have advantages over TSE, there are factors that favor one approach over the other. Both TSE-SSFP and T2P-SSFP provide bright-blood contrast, which has been shown to improve diagnostic confidence over dark-blood TSE for detecting T2 abnormalities associated with acute myocardial infarction (11). TSE-SSFP and T2P-SSFP use gradient moment nulling and thus eliminate the need for the double inversion recovery preparation that causes myocardial signal losses (11).

TSE-SSFP clearly has benefits over T2P-SSFP with regard to SNR and CNR. With an SSFP readout and 90° RF pulses only $M_{xy} = M_o\cos(45°)$ is sampled in contrast to TSE where $M_{xy} = M_o$. Also, the T2-weighted magnetization that is stored along the longitudinal axis at the end of the T2 preparation decays according to T1, resulting in further signal loss. Differences between phantom and in vivo SNR data suggest that T2P-SSFP may suffer from signal losses in vivo. While the use of composite 180° RF pulses and an MLEV (20) scheme in the T2 preparation may partially compensate for RF pulse imperfections, it has been shown that adiabatic refocusing pulses may be beneficial (27) for compensating for signal losses due to off-resonance. Additional adiabatic excitation at the beginning and adiabatic storing of the magnetization at the end of the T2 preparation may reclaim some of the lost signal. Because TSE-SSFP does not use a T2 preparation, this type of signal loss does not occur.

On the other hand, T2P-SSFP provides more accurate measurements of T2 than TSE-SSFP or TSE. The T2 contrast for edema imaging was mainly derived from the T2 preparation while the SSFP readout with a flip angle of 90° was used as a fast method for acquiring the image. T2P-SSFP has been recently applied with single-shot imaging, which is beneficial in patients with arrhythmias or with difficulty breathholding (11). In this prior clinical study, it was shown that, when combined with motion-corrected averaging, these methods yield a $\sqrt{8}$-fold improvement in SNR (eight images total averaged). Such single-shot approaches may be also applicable to TSE-SSFP but T2P-SSFP should possess a better point-spread function than TSE-SSFP or TSE, because it has more uniform T2-weighting across k-space.

Limitations

With the current implementation at 1.5T, the use of 180° RF pulses throughout the TSE-SSFP single cardiac phase readout results in RF-specific absorption ratios within Food and Drug Administration (FDA) specified limits (whole-body specific absorption rate [SAR] of 0.88 W/kg measured for 200-lb patient weight and 2RR repetition with RR interval of 800 ms). Given that SAR quadruples at 3T, it is expected that TSE-SSFP can be used at higher field strengths, because FDA guidelines limit SAR whole-body exposure to 4.0 W/kg. However, it is likely that RF-specific absorption ratio limits may prohibit the use of TSE-SSFP in continuous multi-phase cine imaging in a similar manner to that of TSE, which also is not used for cine imaging.

Fat suppression with TSE-SSFP was not explored as part of this work. This was done so that SNR measurements would not be influenced by potential imperfections in the implementation of the fat-suppression methods. However, both chemical shift and inversion-based methods are in-

herently compatible with TSE-SSFP. Although fat suppression is commonly combined with T2-weighted methods, it is not strictly required for imaging myocardial edema secondary to acute myocardial infarction, because fat can usually be distinguished from transmurally edematous myocardium localized in and around the infarcted zone. Moreover, chemical shift fat saturation methods in the presence of static field inhomogeneity (e.g., due to sternal wires or stents) can result in direct myocardial suppression artifacts. Last, inversion based fat suppression introduces unwanted signal loss and T1-weighting.

SNR, CNR, and T2 quantification with TSE-SSFP may be affected by B1 transmit inhomogeneity, slice profile and imperfect refocusing due to flip angle imperfections. These factors will require additional study.

REFERENCES

1. Hennig J, Nauerth A, Friedburg H. RARE imaging: a fast imaging method for clinical MR. Magn Reson Med 1986;3:823–833.
2. Marie PY, Angioi M, Carteaux JP, et al. Detection and prediction of acute heart transplant rejection with the myocardial T2 determination provided by a black-blood magnetic resonance imaging sequence. J Am Coll Cardiol 2001;37:825–831.
3. Abdel-Aty H, Zagrosek A, Schulz-Menger J, et al. Delayed enhancement and T2-weighted cardiovascular magnetic resonance imaging differentiate acute from chronic myocardial infarction. Circulation 2004;109: 2411–2416.
4. Abdel-Aty H, Boye P, Zagrosek A, et al. Diagnostic performance of cardiovascular magnetic resonance in patients with suspected acute myocarditis: comparison of different approaches. J Am Coll Cardiol 2005;45:1815–1822.
5. Aletras AH, Tilak GS, Natanzon A, et al. Retrospective determination of the area at risk for reperfused acute myocardial infarction with T2-weighted cardiac magnetic resonance imaging: histopathological and displacement encoding with stimulated echoes (DENSE) functional validations. Circulation 2006;113:1865–1870.
6. Kim RJ, Fieno DS, Parrish TB, et al. Relationship of MRI delayed contrast enhancement to irreversible injury, infarct age, and contractile function. Circulation 1999;100:1992–2002.
7. Simonetti OP, Finn JP, White RD, Laub G, Henry DA. "Black blood" T2-weighted inversion-recovery MR imaging of the heart. Radiology 1996;199:49–57.
8. Pennell D. Myocardial salvage: retrospection, resolution, and radio waves. Circulation 2006;113:1821–1823.
9. Keegan J, Gatehouse PD, Prasad SK, Firmin DN. Improved turbo spin-echo imaging of the heart with motion-tracking. J Magn Reson Imaging 2006;24:563–570.
10. Oppelt A, Graumann R, Fischer H, Hartl W, Schajor W. FISP-a new fast MRI sequence. Electromedica 1986;54:15–18.
11. Kellman P, Aletras AH, Mancini C, McVeigh ER, Arai AE. T2-prepared SSFP improves diagnostic confidence in edema imaging in acute myocardial infarction compared with turbo spin echo. Magn Reson Med 2007;57:891–897.
12. Brittain JH, Hu BS, Wright GA, Meyer CH, Macovski A, Nishimura DG. Coronary angiography with magnetization-prepared T2 contrast. Magn Reson Med 1995;33:689–696.
13. Deimling M, Heid O. Magnetization prepared true FISP imaging. Proceeding of Society of Magnetic Resonance, 2nd Annual Scientific Meeting. August 6, 1994; San Francisco. p 495.
14. Deshpande VS, Chung YC, Zhang Q, Shea SM, Li D. Reduction of transient signal oscillations in true-FISP using a linear flip angle series magnetization preparation. Magn Reson Med 2003;49:151–157.
15. Hennig J, Speck O, Scheffler K. Optimization of signal behavior in the transition to driven equilibrium in steady-state free precession sequences. Magn Reson Med 2002;48:801–809.
16. Hahn EL. Spin echoes. Phys Rev 1950;80:580–594.
17. Hinks RS, Constable RT. Gradient moment nulling in fast spin echo. Magn Reson Med 1994;32:698–706.
18. Paul D, Markl M, Fautz HP, Hennig J. T2-weighted balanced SSFP imaging (T2-TIDE) using variable flip angles. Magn Reson Med 2006; 56:82–93.
19. Huang TY, Huang IJ, Chen CY, Scheffler K, Chung HW, Cheng HC. Are TrueFISP images T2/T1-weighted? Magn Reson Med 2002;48:684–688.
20. Levitt M, Freeman R, Frenkiel T. Supercycles for broadband heteronuclear decoupling. J Magn Reson 1982;50:157–160.
21. Nazarova I, Hemminga MA. Analytical analysis of multi-pulse NMR. J Magn Reson 2004;170:284–289.
22. Messroghli DR, Plein S, Higgins DM, et al. Human myocardium: single-breath-hold MR T1 mapping with high spatial resolution—reproducibility study. Radiology 2006;238:1004–1012.
23. Constantinides CD, Atalar E, McVeigh ER. Signal-to-noise measurements in magnitude images from NMR phased arrays. Magn Reson Med 1997;38:852–857.
24. Boyle GE, Ahern M, Cooke J, Sheehy NP, Meaney JF. An interactive taxonomy of MR imaging sequences. Radiographics 2006;26:e24; quiz e24.
25. Fransson A, Ericsson A, Jung B, Sperber GO. Properties of the phase-alternating phase-shift (PHAPS) multiple spin-echo protocol in MRI: a study of the effects of imperfect RF pulses. Magn Reson Imaging 1993; 11:771–784.
26. Constable RT, Anderson AW, Zhong J, Gore JC. Factors influencing contrast in fast spin-echo MR imaging. Magn Reson Imaging 1992;10: 497–511.
27. Nezafat R, Stuber M, Ouwerkerk R, Gharib AM, Desai MY, Pettigrew RI. B1-insensitive T2 preparation for improved coronary magnetic resonance angiography at 3 T. Magn Reson Med 2006;55:858–864.
28. Haacke EM, Brown RW, Thompson MR, Venkatesan R. Magnetic resonance imaging: physical principles and sequence design. New York: John Wiley & Sons; 1999. 480 p.